

**A Two-Stage Light Gas Gun for the
Study of High Speed Impact in
Propellants**

Con Doolan

DSTO-TR-1092

DISTRIBUTION STATEMENT A
Approved for Public Release
Distribution Unlimited

20010419 032

A Two-Stage Light Gas Gun for the Study of High Speed Impact in Propellants

Con Doolan

**Weapons Systems Division
Aeronautical and Maritime Research Laboratory**

DSTO-TR-1092

ABSTRACT

This report describes a proposed two-stage light gas gun for the investigation of high speed impact in solid rocket propellants. Such a facility would provide valuable, quantitative information on the IM response of propellants for the ADF. A description of the operating principles and anticipated design is followed by a performance prediction using a numerical model. A quasi-one-dimensional computational fluid dynamics code was utilised to simulate the interaction of the gas dynamics with piston and projectile motion. Various projectile masses and initial gas fill pressures were investigated. It was concluded that the device described in this report was capable of accelerating masses of the order of 5-15g at hypervelocity speeds using a helium driver gas and that performance would be enhanced by evacuating the launch tube prior to projectile release. Marginal performance increases could be obtained by replacing the driver gas with hydrogen.

RELEASE LIMITATION

Approved for public release

DEPARTMENT OF DEFENCE
DEFENCE SCIENCE & TECHNOLOGY ORGANISATION

DSTO

AQ FOI-07-1349

Published by

*DSTO Aeronautical and Maritime Research Laboratory
PO Box 1500
Salisbury South Australia 5108 Australia*

*Telephone: (08) 8259 5555
Fax: (08) 8259 6567
© Commonwealth of Australia 2001
AR-011-669
January 2001*

APPROVED FOR PUBLIC RELEASE

A Two-Stage Light Gas Gun for the Study of High Speed Impact in Propellants

Executive Summary

The response of solid rocket propellants to unplanned stimuli can be catastrophic, resulting in loss of personnel and expensive military platforms. Understanding this response is important for the ADF in terms of operations and design/purchase of new weapon systems. Unplanned stimuli can include heat, electrostatic discharge and impact from bullet attack, fragments from sympathetic detonation of nearby rounds or shaped jets from attacking warheads. To date, knowledge of the response of munitions to these stimuli are still not fully understood and there is a lack of a comprehensive model describing the physics of the situation.

Of particular interest is the response of propellants to high speed impact. This can result in various forms of burning, explosion or detonation of the propellant. This report describes a proposed two-stage light gas gun that can accelerate projectiles to hypervelocity speeds ($1-4 \text{ kms}^{-1}$) for the study of impact in rocket propellants. The general operating principles are explained along with a brief description of the facility design. Numerical modelling is performed using a quasi-one-dimensional fluid dynamics code. This enables performance prediction through the simulation of the gas dynamics within the gas gun along with the interactions of the gas volumes, piston and projectile. Results for a helium driver gas and projectile masses in the range of 5-15g are presented and prove the feasibility of the design. Information on the gas, piston and projectile dynamics are presented for a typical operating condition. It was found that significant increases in performance could be achieved by evacuating the launch tube prior to projectile release. The use of hydrogen as a driver gas was also investigated and it was found that, for this configuration, performance increases were marginal and did not justify the increase in risk to operators.

Authors

Con Doolan

Weapons Systems Division

Dr Con Doolan graduated from the University of Queensland in 1992 with a Bachelor of Mechanical Engineering. He later conducted research on hypervelocity wind tunnels and was awarded a Doctor of Philosophy in 1997. Dr Doolan joined DSTO in 2000 after working at the University of Glasgow on helicopter aerodynamics. He now performs research on missile propulsion systems for the ADF and has interests in rocket motor insensitive munitions response and advanced propulsion systems.

Contents

1. INTRODUCTION	1
2. GENERAL OPERATING PRINCIPLES	2
3. FACILITY DESIGN	6
4. NUMERICAL MODELLING	10
4.1 Code Description	10
4.2 Computational Mesh	11
4.3 Numerical Results	11
5. SUMMARY	17
6. REFERENCES	18

Nomenclature

A	Internal area of facility (m^2).
a	Speed of sound in gas (ms^{-1}).
c	Speed of sound in facility wall (ms^{-1}).
E	Young's Modulus (Pa).
L_t	Length of launch tube (m).
M	Projectile Mach number.
m	Mass (kg).
P	Stress (Pa).
p	Pressure (Pa).
R	Gas constant ($\text{Jkg}^{-1}\text{K}^{-1}$), Impedance ratio.
T	Temperature (K).
t	time (s).
U_R	Relative velocity of cell interface (ms^{-1}).
u	Velocity (ms^{-1}).
V	Volume (m^3).
x	Position (m).
γ	Ratio of specific heats.
λ	Compression ratio.
ρ	Density (kgm^{-3}).

Superscripts and subscripts

0	Driver gas, ambient conditions (at 297 K).
1	Initial condition.
2	Post compression.
BURST	Diaphragm burst pressure.
D	Driver.
D_f	Driver fill.
<i>exit</i>	Launch tube exit.
i	i th control mass/cell.
<i>impact</i>	velocity at impact upon compression tube buffer.
j	j th time interval.
LT	Launch tube fill.
MAX	Maximum.
p	Projectile.
<i>pist</i>	Piston.
R_f	Reservoir fill.

1. Introduction

Understanding the impact sensitivity of solid rocket propellants to high speed impact is important in characterising the safety of in-service and new propulsion systems for the ADF. Knowledge of the insensitive munitions (IM) response of these propellants directly affects military operations and how munitions are stored and transported. Apart from generalised models, little is available to guide those assessing the IM response of propulsion systems to high speed ($>1 \text{ kms}^{-1}$) threats. Typically, full scale testing can be performed, or the relative characterisation using tests such as impact weights or explosive card-gap tests. These tests are important for screening and qualification of energetic material, however do not provide detailed quantitative information to build accurate models of important processes such as deflagration-to-detonation transition (DDT) and delayed detonation (XDT).

In order to study the response of propellants to high speed impact in the laboratory, a repeatable system that delivers small fragments of hypervelocity metal needs to be developed. Small quantities of propellant should ideally be used in order to reduce the complexity of the experiments and to enable repetition, which will increase the accuracy of the results. A two-stage light gas gun is ideally suited to this purpose as it can reproduce, in a repeatable and relatively low cost manner, the projectile velocities likely to be encountered by energetic materials during high speed projectile/fragment impact and sympathetic detonation ($1\text{-}4 \text{ kms}^{-1}$).

Two-stage light gas guns have been used extensively for the study of high speed aeroballistics and impact dynamics in the hypervelocity flight regime (see, for example, Zakraysek *et al*, 1999). Conventional powder guns have been used for impacts up to approximately 2 kms^{-1} in solid rocket propellants (Moulard, 1981). In other studies, flyer plate technology has been used for shock-to-detonation-transition (SDT), DDT and XDT studies. Flyer plates can be driven by conventional powder or single-stage gas guns (Wang *et al*, 1998) or explosive charges (Tanaka *et al*, 1999). While flyer plate velocities can be varied widely by choosing different driving modes, experiments are limited to flat plate impact. A two-stage light gas gun will allow projectiles of various geometry to be used at muzzle velocities higher than those achievable by powder guns. Breech and barrel erosion rates are also significantly lower than powder guns as the helium driver gas has very little chemical interaction with the tube walls.

Although used widely in foreign laboratories, Australia currently lacks a hypervelocity gas gun facility to accelerate fragments to 4 kms^{-1} . The development of one at DSTO will fill a technological gap for Australia and may be the only one of its type in the region. Therefore, knowledge gained from experiments using the two-stage light gas gun could give the ADF an operational advantage in terms of threat-hazard analyses and IM response.

2. General Operating Principles

A gas gun differs from a conventional powder gun in that the energy required to accelerate the projectile is derived from a compressed gas reservoir rather than the combustion of a propellant charge. Quantitative studies of the gas gun (e.g. Seigel, 1965) have shown that reducing the molecular weight of the propelling gas can increase projectile muzzle velocity. This is because the gas must accelerate itself along with the projectile. In fact, a simple analysis (Seigel, 1965) will show that the maximum theoretical muzzle velocity is directly related to the speed of sound in the driving chamber,

$$u_{p\max} = \frac{2}{\gamma - 1} a_o \quad (1)$$

Hence by reducing the molecular weight, the speed of sound increases and a higher muzzle velocity is achieved. Further increases in muzzle velocity can be realised by heating the driving gas. Many different methods can be used to heat the driver gas, such as combustion, arc heating or detonation. In the two-stage light gas gun, the driving gas is heated by free-piston compression in a tube mounted upstream of the barrel. Free-piston compression has been used extensively for propellant gas heating (Charters, 1987, Stilp, 1987) and also successfully for driving shock waves in hypervelocity shock tunnels (Stalker, 1967) and expansion tubes (Doolan and Morgan, 1999).

The two stages of operation are illustrated in the schematic shown in Fig. 1. The first stage uses a compressed air reservoir to propel a piston into a tube that contains a light driver gas such as helium. The piston is of sufficient mass so that the helium compression is achieved at a relatively slow rate for the driver gas to be compressed polytropically with no shock wave formation. The piston compresses the gas 40 to 100 times smaller than its initial volume. This process creates very high temperatures. The second stage begins when the driver gas reaches the desired driving pressure. At this point, a diaphragm bursts, allowing the driver gas to accelerate the projectile to high velocity.

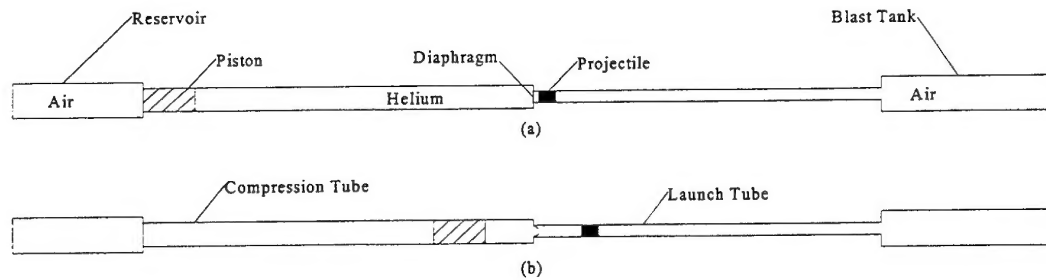


Figure 1. Schematic of two-stage light gas gun operation; (a) Initial state before shot; (b) Piston compresses helium to high pressure, bursts diaphragm and launches projectile.

The performance increase by using compressive heating can be better understood through the results of a simple analysis. If ideal gas behaviour is assumed, the pressure-volume relationship can be described by,

$$p_1 V_1^\gamma = p_2 V_2^\gamma \quad (2)$$

$$p = \rho RT \quad (3)$$

The compression ratio of the driver gas can be defined as the ratio of the initial and final volumes,

$$\lambda = V_1 / V_2 \quad (4)$$

Combining equations (2), (3) and (4) and assuming the speed of sound is related to the root of the temperature,

$$\frac{a_2}{a_1} = \lambda^{\frac{\gamma-1}{2}} \quad (5)$$

Equation (5) gives the theoretical speed of sound increase in the driver gas for a given compression ratio and is plotted in Fig. 2 for monatomic and diatomic driver gases. Figure 2 indicates that considerable increases in sound speed can be achieved and therefore higher muzzle velocities can be obtained (Equation (1)) by using the free-piston compression technique.

It should also be noted that the free-piston compressor is a convenient way of achieving the high pressures required to launch the projectiles. It would be considerably more difficult to construct apparatus based on conventional pumps and compressors to achieve and store the high pressures required for hypervelocity launch.

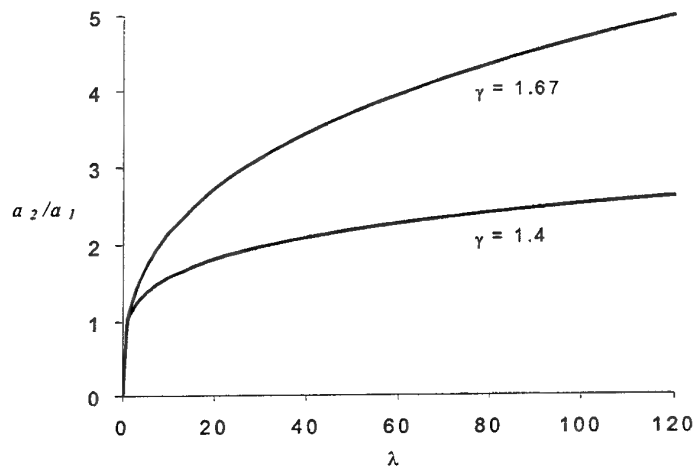


Figure 2. Theoretical speed of sound increase due to piston compression.

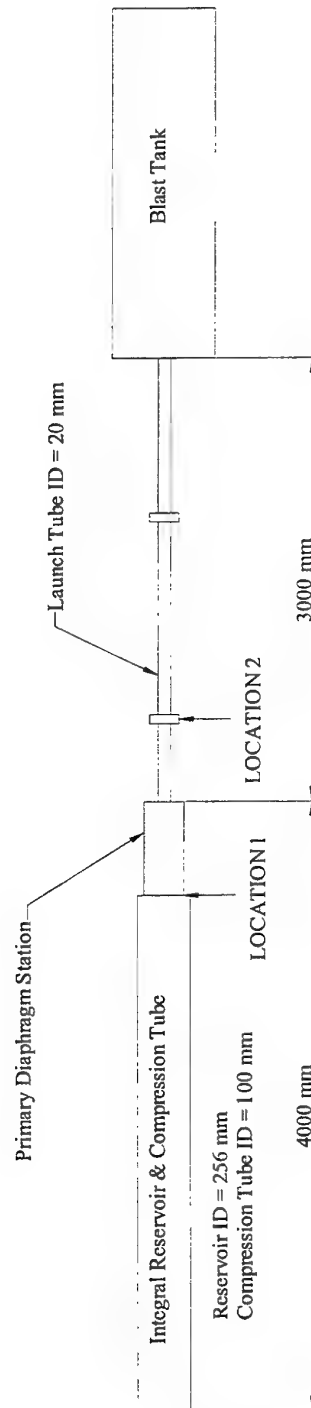


Figure 3. Schematic of the two-stage light gas gun.

The free-piston compressor design used here differs from conventional two-stage light gas guns. In very high performance guns, a deformable piston is used in the breech in order to maintain a high pressure behind the projectile. The piston has a high residual velocity after the projectile is launched and is typically allowed to extrude into a specially designed internal cavity within the breech. Although this design is very successful in attaining high muzzle velocities (up to 12 kms^{-1}), it is an expensive and time consuming process to extract and fabricate pistons for each shot. In the present configuration operation and costs are improved by using a fully reusable piston. Final muzzle velocities are somewhat lower, however performance can be optimised by proper selection of operating conditions to 'tune' the piston motion. By selecting the right combination of reservoir and driver fill pressures along with diaphragm burst pressure and projectile mass, maximum muzzle velocity can be obtained with minimal residual piston velocity at the end of its stroke. Performance can be predicted using analytical and numerical techniques. Section 4 summarises a quasi-one-dimensional numerical technique, which is used to analyse the two-stage light gas gun facility.

3. Facility Design

The two-stage light gas gun is a medium sized facility to be housed on the Explosives Ordnance Precinct at DSTO Salisbury. A sketch of the facility is shown in Fig. 3, which indicates the major dimensions of the important components. The free-piston driver section consists of an integrated design where the air reservoir is constructed as an annular chamber around the compression tube. The piston is held initially in a launcher tube and upon firing, the reservoir gas flows through the launcher and into the compression tube thereby accelerating the piston along the compression tube. The piston compresses the driver gas into a volume just upstream of the primary diaphragm. In this region, the light compression tube is replaced by a heavy walled breech that contains the high pressure driver gas. The maximum design pressure of the breech is 200 MPa, while the reservoir is designed for 15 MPa.

The launch tube consists of 4340 alloy steel tubes with a combined length of 3 m. The blast tank is a heavy walled vessel capable of withstanding detonations of energetic material. For the current configuration, the tank will be registered to withstand a blast equivalent to a 25g TNT detonation. This will allow 50-100g of solid rocket propellant to be used with safety inside the blast tank. Instrumentation for the facility will include piezoelectric pressure transducers to measure transient pressures at various locations along the gas gun and imbedded polyvinylidene fluoride (PVDF) piezofilm shock sensors to measure the impact pressures within the test articles.

The whole facility is mounted on rollers, which eliminates the need for a large recoil energy absorption mechanism. By allowing the gas gun to move freely over 100 mm,

the large reaction forces will cancel out due to the action of the piston increasing the pressure in the breech and reducing the overall facility acceleration.

An important part of the design involves accounting for the dynamic loads, which occur during the rapid compression of the driver gas. The compression occurs faster than the time it takes relieving stress waves to arrive from the free ends of the facility. This means a component of the axial load generated at the primary diaphragm station by rapid piston compression is transmitted throughout the light gas gun. This load can be determined using a numerical stress wave analysis technique which is summarised below.

The dynamic stress analysis procedure used here is based on one-dimensional stress wave theory (Zukas *et al*, 1982). The model relies upon the conservation of momentum and energy for the analysis of stress levels. To calculate pressure changes within the facility walls, the model uses the basic dynamic stress wave equation,

$$\Delta P = \rho c \Delta u \quad (6)$$

where c , the speed of sound in the material, is given by,

$$c = \sqrt{\frac{E}{\rho}} \quad (7)$$

Dynamic stress levels can be calculated by using a numerical technique where the facility is discretized into a number of mass control points each possessing the attributes of length, area, density and Young's modulus. For the two-stage light gas gun, the facility is approximated by the sections shown in Table 1 below in order to simplify the analysis procedure.

Table 1. Sections used for dynamic stress analysis of the light gas gun.

Description	Area (m ²)	Length (m)
Launch tube	0.0054	3
Primary diaphragm station	0.0412	0.640
Reservoir tube	0.0177	3.51
Launcher end cap	0.0491	0.05

Once the facility is represented as a collection of discrete control masses, boundary conditions can be applied and temporal axial stress can be determined at any location by cycling through the numerical scheme. Free-stress ($P=0$) boundary conditions are used for launcher and muzzle ends. At the approximate location of the primary diaphragm, the pressure is specified which simulates the dynamic piston compression of the driver gas. The loading condition used for the stress wave simulations is a

symmetrical triangular load which has a ramp-like rise to 200 MPa in 1.6 ms and a ramp-like fall to zero load in 1.6 ms.

After application of the boundary conditions and driving pressure, the change in velocity for each control mass can be calculated. This done using a first order integration of Newton's second law,

$$u_i^{j+1} = u_i^j + \frac{(P_i^j A_i + P_{i+1}^j A_{i+1})}{m_i} dt \quad (8)$$

Once new velocities are calculated, interface pressures between the cells can be determined. The change in velocity (Δu) must be determined in a reference frame relative to the interface between each cell. This reference frame includes a term for impedance changes across the interface due to area and material variations,

$$U_R = \frac{R u_i^j + u_{i+1}^j}{1 + R} \quad (9)$$

where

$$R = \frac{A_i \rho_i c_i}{A_{i+1} \rho_{i+1} c_{i+1}} \quad (10)$$

Pressure change at the interface is calculated using,

$$P_i^{j+1} = P_i^j + \rho_i c_i (U_R - u_i^{j+1}) \quad (11)$$

After the new pressures are calculated, the time can be advanced by a small increment and the cycle repeated. For this numerical scheme, in order for the correct wave speed to be maintained, the time-step and cell length must be kept in the ratio,

$$2c = \frac{dx}{dt} \quad (12)$$

The results of a dynamic stress simulation are presented below. In this case, the material is assumed to be steel throughout, with a density of 7800 kgm⁻³ and a Young's Modulus of 207 GPa. The sound speed is 5150 ms⁻¹ and the cell length is 1 mm and therefore from equation (12), the time step is 0.097 ms. The cell length was determined by performing simulations on a simple steel bar given a 1 ms⁻¹ impact. Transient stress results were compared with one-dimensional theory and the cell length was systematically reduced until the results were of acceptable accuracy.

The transient stress levels at two locations (shown in Fig. 3) are presented. These locations are:

1. The location of the connecting flange between the reservoir and primary diaphragm collar.
2. The location of the first connecting flange in the launch tube (285 mm downstream of the primary diaphragm).

These are considered two of the most critical locations in the facility, as separation of the components here would cause major damage to the laboratory. Figures 4 and 5 show the calculated transient stresses in the locations. Positive stress indicates tension while negative stress indicates compression. The stress history generally follows the intensity of the pressure loading and leaves behind a low level stress oscillation, which would be expected to quickly attenuate due to internal friction.

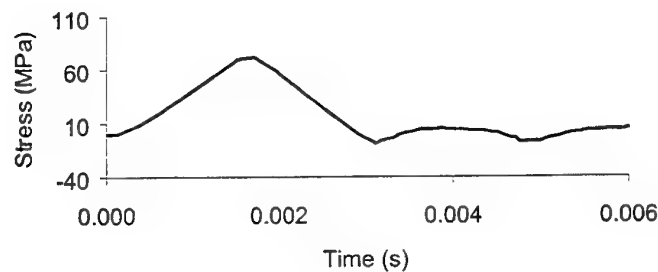


Figure 4. *Dynamic axial stress at joint between reservoir and primary diaphragm collar (Location 1, Fig. 3).*

In Fig. 5, a high compressive loading is experienced in the launch tube flange. As the load is compressive it will not separate the flange and therefore is not expected to compromise its structural integrity. The residual transient stresses have a tensile component, and the flange must be designed to cope with these. The launch tubes will be made from a high tensile, low alloy steel that should easily withstand the applied loading.

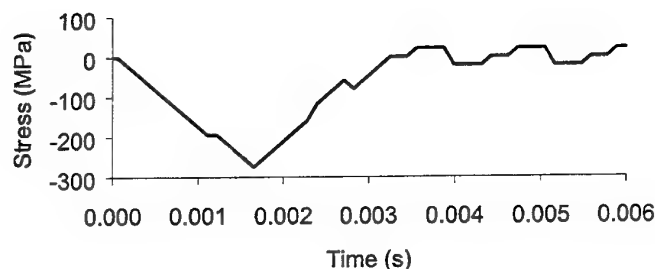


Figure 5. Dynamic axial stress at first connecting flange in the launch tube (Location 2, Fig. 3).

4. Numerical Modelling

4.1 Code Description

The anticipated performance of the gas gun has been modelled using a quasi-one-dimensional computational fluid dynamics code (Jacobs, 1994). In this method, the gas dynamic equations are solved by discretizing the various regions of gas within the facility. The regions or 'slugs' of gas are the reservoir gas (compressed air which pushes the piston), the driver gas (gas in front of the piston which is compressed and eventually accelerates the projectile) and the air in front of the projectile in the launch tube. The numerical modelling is based on a Lagrangian formulation of the gas dynamics where each cell is treated as a point mass. At the interfaces between the cells pressures and velocities are calculated using an approximate Riemann solver (Jacobs, 1992).

The code has the ability to simulate the interaction of several gas slugs, pistons, diaphragms and projectiles making it very useful in the study of free-piston driven gas gun and shock tube facilities. Coupling of the gas slugs to the pistons and diaphragms is achieved by the proper selection of boundary conditions. Viscous effects are included using standard engineering correlations for friction and heat transfer in pipe flow. Although these correlations are derived for steady incompressible flow, results using this code (Jacobs, 1994) indicate remarkable performance in flows which are predominately compressible and unsteady. The code also allows area changes that are assumed to occur gradually over finite distances. The reader is referred to Jacobs (1994), Doolan and Jacobs (1996), Tani *et al* (1994) and Maus *et al* (1992) for further information on the quasi-one-dimensional numerical technique.

4.2 Computational Mesh

The computational domain is divided into the reservoir, the compression tube and launch tube. Separating the reservoir gas and the driver gas is the piston and similarly, the projectile separates the driver gas and the air which is initially within the launch tube. To simulate the bursting of the diaphragm, which launches the projectile, the situation is simplified to one where the projectile is held until a specified release pressure is obtained on the upstream side of the projectile. The release pressure is identical to the dynamic burst pressure of the diaphragm.

Table 2 gives a summary of the individual component dimensions. In the following simulations the reservoir gas is compressed air, the driver gas is either helium or hydrogen and the initial air pressure in the launch tube is varied in order to understand the influence of the gas dynamics downstream of the projectile.

Table 2. Summary of component dimensions.

Component	Diameter (mm)	Length (mm)	Mass (kg)
Reservoir	142.8	3000	-
Compression Tube	100	3225	-
Piston	100	225	15
Launch Tube	20	3000	-
Projectile	20	20	$5 \times 10^{-3}, 10 \times 10^{-3}, 15 \times 10^{-3}$

In order to achieve an accurate numerical result, cells are distributed throughout the various gas slugs in a way which reflects the relative importance of resolving the gas dynamics. The resolution is as follows: 100 cells in the reservoir tube and 400 in each of the compression and launch tubes. The cells in the reservoir tube are clustered towards the piston to increase the accuracy of the piston dynamics.

It is important to determine the adequacy of the computational mesh in resolving the gas gun flow. For accuracy considerations, a limited number of tests were performed where the number of cells was doubled in each gas slug. It was found that after comparing the results of the two grid resolutions the differences in calculated muzzle exit velocity and peak driver gas pressure were 0.046% and 0.35% respectively. It was therefore concluded that the numerical mesh stated above provided sufficient numerical resolution and accuracy.

4.3 Numerical Results

Various simulations were performed using a combination of different reservoir and driver gas fill pressures and projectile launch masses. The effect of reducing the air pressure in the launch tube was also investigated along with varying the release pressure of the projectile (simulating different diaphragm burst pressures). In most

simulations the driver gas was helium, however in a limited number of simulations the driver gas was replaced with hydrogen in order to ascertain the performance change.

In this report performance is measured in terms of muzzle velocity, however another important factor to consider is the peak pressure experienced at the primary diaphragm station. For the current design this must be limited to 200 MPa. The speed at which the piston impacts upon the buffer at the end of the compression tube is also an important parameter to consider. In order to maximise the life of the piston, the impact speed must be kept to a minimum.

Table 3 gives a summary of the numerical simulation results performed for the two-stage light gas gun. The results show that a gas gun in the proposed configuration is capable of producing muzzle exit velocities up to 4 kms⁻¹. However, this can only be achieved by using a light projectile (5g) and by evacuating the launch tube gas from in front of the projectile before launch. When the gas gun is first commissioned, it is planned to use a simpler configuration where the launch tube is not evacuated and to accelerate a heavier projectile (15g) using helium gas. A simulation incorporating these features is shown in Table 3 as run number 7 and this test case will be examined in more detail.

Table 3. Summary of light gas gun numerical results.

Run No.	p_{Rf} (MPa)	p_{Df} (kPa)	Driver Gas	p_{BURST} (MPa)	m_p (g)	p_{LT} (kPa)	u_{exit} (ms ⁻¹)	u_{impact} (ms ⁻¹)	$p_{D,MAX}$ (MPa)
1	3.4	119	He	70	5	101	2334	3.9	76.3
2	3.4	119	He	70	10	101	1938	Rebound	80.96
3	3.4	119	He	70	15	101	1674	Rebound	84.6
4	9	312	He	185	5	101	3346	Rebound	193.4
5	5.2	119	He	70	5	101	2835	30.2	101
6	5.2	119	He	70	10	101	2464	17	121.7
7	5.2	119	He	70	15	101	2188	5.9	138.3
8	7.5	173	He	100	15	101	2562	4	192.2
9	5.2	119	He	80	5	101	2881	27	108.7
10	5.2	119	He	100	5	101	2975	20.7	128.7
11	5.2	119	He	120	5	101	3044	15.2	147.3
12	5.2	119	He	175	5	101	3160	Rebound	196.9
13	9	312	He	185	5	0.4	3968	Rebound	193.4
14	3.4	119	He	70	5	0.4	2816	3	76.3
15	3.4	119	He	70	10	0.4	2157	Rebound	80.9
16	3.4	119	He	70	15	0.4	1807	Rebound	85.4
17	5.2	119	He	70	5	0.4	3377	30.58	100.8
18	5.2	119	He	70	10	0.4	2729	17.34	121.4
19	5.2	119	He	70	15	0.4	2355	6.13	138.1
20	5.2	119	He	80	5	0.4	3441	27.7	108.6
21	5.2	119	He	100	5	0.4	3573	21.9	128.6
22	5.2	119	He	120	5	0.4	3669	15.65	147.2
23	5.2	119	He	175	5	0.4	3839	3	196.7
24	3.4	119	H ₂	70	5	0.4	3122	25.6	97.6
25	3.4	119	H ₂	70	10	0.4	2394	23.9	117.5
26	3.4	119	H ₂	70	15	0.4	2025	1.3	133
27	6.8	240	H ₂	140	5	0.4	4170.7	27.0	196.8

Figure 6 shows colour contours of the logarithm of pressure in (x,t) space for run number seven. The plot shows only the high pressure section of the compression tube

and the launch tube. The piston and projectile trajectories are marked as shown. As the piston approaches the end of the compression tube, the pressure increases to 70 MPa where the projectile is released and then begins to accelerate into the launch tube. The conditions are set so that the piston has enough residual velocity to continue the compression of the helium gas after projectile release. Initially, the rate of piston compression of the helium gas is higher than the rate of expansion due to the projectile motion. This increases and sustains the acceleration of the projectile so a higher muzzle velocity can be achieved. The projectile acceleration increases until the gas velocity at the launch tube entrance becomes sonic and mass flow is 'choked'. The air in front of the projectile is also compressed until it reaches a maximum of 4.87 MPa.

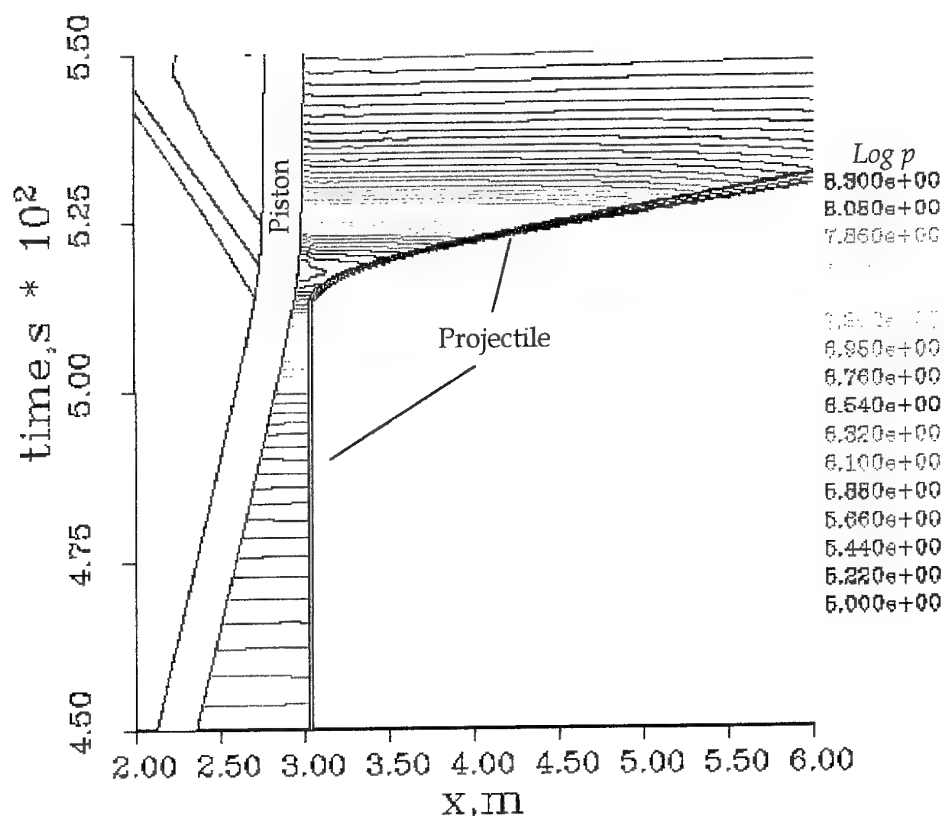


Figure 6. Space-time diagram for simulation run number 7; contours are equally spaced values of $\log p$.

The over-compression of the helium gas in the compression tube not only maximises the projectile velocity but also effectively decelerates the piston and allows it to come to a 'soft landing'. This can only be achieved by careful selection of the reservoir and

driver gas fill pressures along with projectile release pressure (in practise, the diaphragm burst pressure). The incorrect setting of these parameters might cause an impact of the piston at high speed into the compression tube buffer or a piston rebound which may be followed by a high speed impact after the driver gas has drained out of the compression tube. Optimally, the driver gas drains at a rate so that the piston impacts with small residual velocity and no rebounding will occur. When the free-piston driver operates in such a state it is known as 'tuned' piston operation.

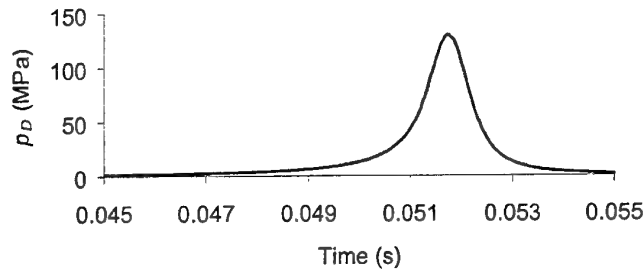


Figure 7. Calculated pressure history of driver gas at the primary diaphragm station.

Figure 7 shows the pressure history of the helium driver calculated just upstream of the initial position of the projectile. The compression is not quite symmetrical, with the slope of the plot changing after the projectile is released after 70 MPa. Considerable over-pressure occurs, and the peak pressure obtained is 138.3 MPa.

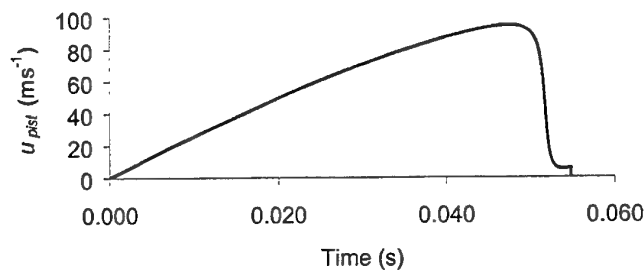


Figure 8. Piston Velocity versus time for run number 7.

Figure 8 displays the expected piston velocity with respect to time. The piston achieves a maximum velocity of 94.7 ms^{-1} . Rapid deceleration occurs due to the over-compression of the helium gas until the piston has a velocity of about 5 ms^{-1} . After this point, most of the driver gas has drained into the launch tube and the residual

reservoir gas pressure now exceeds the driver gas pressure in front of the piston. The piston therefore accelerates slightly into the buffer with an impact velocity of 5.9 ms^{-1} .

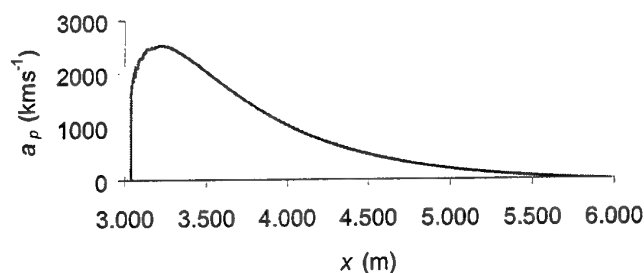


Figure 9. Projectile acceleration versus distance for run number 7.

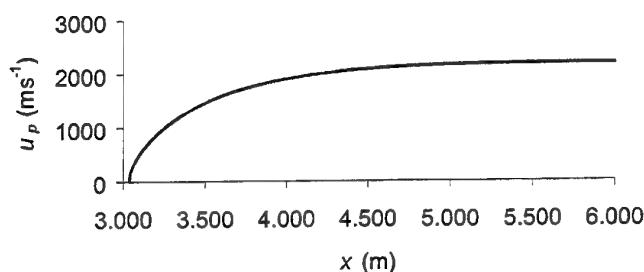


Figure 10. Projectile velocity versus distance for run number 7.

The computed projectile acceleration and velocity for run number 7 are shown in Figs. 9 and 10 respectively. The projectile acceleration increases from $1465 \times 10^3 \text{ ms}^{-2}$ to $2522 \times 10^3 \text{ ms}^{-2}$ as the driver gas is further compressed after piston release. At this point the projectile velocity is such that the flow is becoming choked at the launch tube exit and the piston cannot maintain the mass flow rate behind the projectile. The projectile velocity reaches a constant value of 2188 ms^{-1} towards the end of the launch tube. The air pressure in front of the projectile is also increasing hence the rapid decline in acceleration. The acceleration becomes approximately zero at the launch tube exit.

Evacuating the launch tube prior to projectile release can enhance performance. To investigate this, a number of simulations were performed where the initial launch tube pressure was 400 Pa . The results are shown in Fig. 11 as a normalised performance

chart for the gas gun. The expected performance of the gas gun can be determined by using Fig. 11. For the initial conditions considered in this case, a 7.6% increase in muzzle velocity can be expected when the launch tube is evacuated. More significant gains in can be expected when the performance of the gun is elevated to the $\frac{p_{\max} L_t}{m_p a_o^2} = 1 \times 10^{-6}$ regime (i.e. 200 MPa maximum driver gas pressure and projectile mass 5 g). It is envisaged that the gas gun will initially be commissioned and run with the launch tube cavity at atmospheric pressure. Future development of the facility will incorporate an evacuated launch tube to increase the performance envelope.

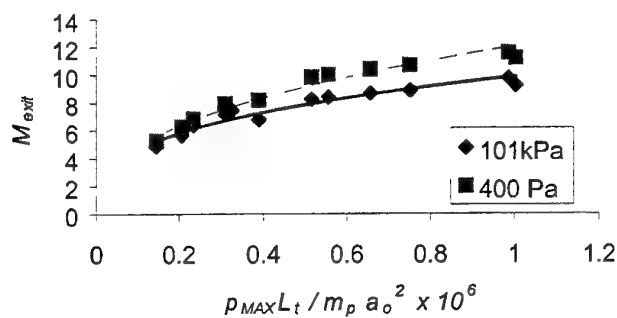


Figure 11. Normalised performance chart for two-stage light gas gun with two initial launch tube pressures, 101 kPa and 400 Pa.

The use of hydrogen as a driving gas was also investigated in a limited number of numerical test cases (Table 3). Results show that an 8.5% increase in muzzle velocity can be expected when the facility is operating at peak performance. The increase risk to personnel and equipment of hydrogen gas outweighs this marginal increase in performance and therefore there are no plans to use it at this stage.

For the results presented above, the friction that occurs between the projectile and the launch tube wall has not been included in the numerical model. Based on experimental results from high speed guns, Seigel (1965) presents a curve whereby muzzle velocity losses can be estimated. Using this information for run number 7 above, the expected loss in muzzle velocity is 3%.

5. Summary

There is a requirement for quantitative data concerning high speed fragment impact of solid rocket propellant. The data is required for insensitive munitions studies for in service and future acquisitions for the ADF and for hazard analyses of future threats. It

is proposed that a two-stage light gas gun be constructed in order to obtain such information. The details of a light gas gun capable of accelerating projectiles to 1-4 kms⁻¹ are presented. Numerical results using a quasi-one-dimensional computational gas dynamics code investigate the processes occurring within the facility and also examine the performance envelope. Results show that eventually it would be advantageous to evacuate the launch tube prior to firing the gas gun, however the first commissioning should be performed with the launch tube at atmospheric pressure. The use of hydrogen as a driving gas was investigated also. It was found that performance increases were possible but the increase in risk was thought to outweigh the expected benefits.

Another benefit of the two-stage light gas gun facility is the ease of re-configuration as a free-piston shock tube. By removing the projectile and filling the launch tube with a low pressure gas, high speed shock waves of the order of 4 kms⁻¹ could be driven through this gas and allow the study of shock wave reflection on propellants. Propulsion systems stored in a naval magazine, for example, could be subjected to a blast wave of similar magnitude in the advent of an unplanned explosive event. In another configuration, propellant samples could be placed at the high pressure end of the free-piston driver and rapidly loaded by gas pressure at rates of the order of 50 GPas⁻¹. This loading rate would simulate the processes that occur during DDT and XDT in propellants and would aid those attempting to understand these complex IM responses.

6. References

- Charters AC (1987) Development of the high-velocity gas-dynamics gun. *Int. J. Impact Engng*, Vol. 5, pp. 183-207.
- Doolan CJ and Morgan RG (1999) A two-stage free-piston driver. *Shock Waves*, Vol. 9, pp. 239-248.
- Doolan CJ and Jacobs PA (1996) Modelling mass entrainment in a quasi-one-dimensional shock tube code. *AIAA J.*, Vol. 34, No. 6, pp. 1291-1293.
- Jacobs (1994) Quasi-one-dimensional modelling of a free-piston shock tunnel. *AIAA J.*, Vol. 32, No. 1, pp. 137-145.
- Jacobs (1992) An approximate Riemann solver for hypervelocity flows. *AIAA J.*, Vol. 30, No. 10, pp. 2558-2561.
- Maus J, Laster M, and Hornung H (1992) The G-Range impulse facility, a high performance free-piston shock tunnel. AIAA Paper 92-3946.

Moulard H (1981) Critical conditions for shock initiation of detonation by small projectile impact. Proceedings Seventh Symposium (International) on Detonation, NSWC, pp. 316-324.

Seigel AE (1965) The theory of high speed guns. AGARDograph 91, NATO.

Stalker RJ (1967) A study of the free-piston shock tunnel. *AIAA J.*, Vol. 5, No. 12, pp. 2160-2165.

Stilp AJ (1987) Review of modern hypervelocity impact facilities. *Int. J. Impact Engng.*, Vol. 5, pp. 613-621.

Tanaka K, Noda K, Hyodo Y, Nakamura H, Kosaka K, Nakayama T, Katayama M and Takeba A (1999) XDT in HTPB propellant from steel flyer plate impact tests. *Shock Compression of Condensed Matter - 1999*, American Institute of Physics, pp. 667-670.

Tani K, Itoh K, Takahashi M, Tanno H, Komuro, H and Miyajima H (1994) Numerical study of free-piston shock tunnel performance. *Shock Waves*, Vol. 3, pp. 313-319.

Wang L, Feng C and Han C (1998) Experimental study on boron-potassium nitrate initiated by shock. *J. Propulsion and Power*, Vol. 14, No. 4, pp. 416-420.

Zakraysek AJ, Sutherland GT, Sandusky HD and Strange D (1999) A new gun facility dedicated to performing shock physics and terminal ballistics experiments. *Shock Compression of Condensed Matter - 1999*, American Institute of Physics, pp. 1091-1094.

Zukas JA, Nicholas T, Swift, HF, Greszczuk, LB and Curran DR (1982) *Impact Dynamics*. Wiley, New York.

DISTRIBUTION LIST

A Two-Stage Light Gas Gun for the Study of High Speed Impact in Propellants

Con Doolan

AUSTRALIA

DEFENCE ORGANISATION

Task Sponsor DGNAVSYS

S&T Program

Chief Defence Scientist	} shared copy
FAS Science Policy	
AS Science Corporate Management	
Director General Science Policy Development	
Counsellor Defence Science, London (Doc Data Sheet)	
Counsellor Defence Science, Washington (Doc Data Sheet)	
Scientific Adviser to MRDC Thailand (Doc Data Sheet)	
Scientific Adviser Policy and Command	
Navy Scientific Adviser	
Scientific Adviser - Army (Doc Data Sheet and distribution list only)	
Air Force Scientific Adviser	
Director Trials	

Aeronautical and Maritime Research Laboratory

Director

Chief of Weapons Systems Division
Research Leader: RLMWS Dave Thomson
Head: PST Sook Ying Ho
Author(s): Con Doolan (4 Copies)

DSTO Library and Archives

Library Fishermans Bend
Library Maribyrnong (Doc Data Sheet)
Library Salisbury
Australian Archives
Library, MOD, Pyrmont (Doc Data sheet only)
US Defense Technical Information Center, 2 copies
UK Defence Research Information Centre, 2 copies
Canada Defence Scientific Information Service, 1 copy
NZ Defence Information Centre, 1 copy
National Library of Australia, 1 copy

Capability Systems Staff

Director General Maritime Development
Director General C3I Development (Doc Data Sheet only)
Director General Aerospace Development (Doc Data Sheet only)

Navy

SO (Science), Director of Naval Warfare, Maritime Headquarters Annex,
Garden Island, NSW 2000. (Doc Data Sheet only)
LCDR Adrian O'Donoghue, Armament Section (Explosive Ordnance Systems),
Directorate of Naval Weapons Systems, CP4-7-159
Campbell Park Offices Canberra ACT 2600

Army

ASNSO ABCA, Puckapunyal, (4 copies)
SO (Science), DJFHQ(L), MILPO Enoggera, Queensland 4051 (Doc Data Sheet
only)

Intelligence Program

DGSTA Defence Intelligence Organisation
Manager, Information Centre, Defence Intelligence Organisation

Corporate Support Program

Library Manager, DLS-Canberra

UNIVERSITIES AND COLLEGES

Australian Defence Force Academy
Library
Head of Aerospace and Mechanical Engineering
Serials Section (M list), Deakin University Library, Geelong, 3217
Hargrave Library, Monash University (Doc Data Sheet only)
Librarian, Flinders University

OTHER ORGANISATIONS

NASA (Canberra)
Aus Info

OUTSIDE AUSTRALIA**ABSTRACTING AND INFORMATION ORGANISATIONS**

Library, Chemical Abstracts Reference Service
Engineering Societies Library, US
Materials Information, Cambridge Scientific Abstracts, US
Documents Librarian, The Center for Research Libraries, US

INFORMATION EXCHANGE AGREEMENT PARTNERS

Acquisitions Unit, Science Reference and Information Service, UK
Library - Exchange Desk, National Institute of Standards and Technology, US

SPARES (5 copies)

Total number of copies: 50

DEFENCE SCIENCE AND TECHNOLOGY ORGANISATION DOCUMENT CONTROL DATA					
				1. PRIVACY MARKING/CAVEAT (OF DOCUMENT)	
2. TITLE A Two-Stage Light Gas Gun for the Study of High Speed Impact in Propellants			3. SECURITY CLASSIFICATION (FOR UNCLASSIFIED REPORTS THAT ARE LIMITED RELEASE USE (L) NEXT TO DOCUMENT CLASSIFICATION) Document (U) Title (U) Abstract (U)		
4. AUTHOR(S) Con Doolan			5. CORPORATE AUTHOR Aeronautical and Maritime Research Laboratory PO Box 1500 Salisbury SA 5108 Australia		
6a. DSTO NUMBER DSTO-TR-1092		6b. AR NUMBER AR-011-669		6c. TYPE OF REPORT Technical Report	
				7. DOCUMENT DATE January 2001	
8. FILE NUMBER J 9505/19/226	9. TASK NUMBER NAV 00/107	10. TASK SPONSOR DGNAVSYS	11. NO. OF PAGES 20	12. NO. OF REFERENCES 15	
13. URL ON THE WORLD WIDE WEB http://www.dsto.defence.gov.au/corporate/reports/DSTO-TR-1092.pdf			14. RELEASE AUTHORITY Chief, Weapons Systems Division		
15. SECONDARY RELEASE STATEMENT OF THIS DOCUMENT <i>Approved for public release</i>					
OVERSEAS ENQUIRIES OUTSIDE STATED LIMITATIONS SHOULD BE REFERRED THROUGH DOCUMENT EXCHANGE, PO BOX 1500, SALISBURY, SA 5108					
16. DELIBERATE ANNOUNCEMENT No Limitations					
17. CASUAL ANNOUNCEMENT Yes					
18. DEFTTEST DESCRIPTORS Light gas guns, Hypervelocity impact, Hypervelocity projectiles, Solid rocket propellants, Mathematical models					
19. ABSTRACT This report describes a proposed two-stage light gas gun for the investigation of high speed impact in solid rocket propellants. Such a facility would provide valuable, quantitative information on the IM response of propellants for the ADF. A description of the operating principles and anticipated design is followed by a performance prediction using a numerical model. A quasi-one-dimensional computational fluid dynamics code was utilised to simulate the interaction of the gas dynamics with piston and projectile motion. Various projectile masses and initial gas fill pressures were investigated. It was concluded that the device described in this report was capable of accelerating masses of the order of 5-15g at hypervelocity speeds using a helium driver gas and that performance would be enhanced by evacuating the launch tube prior to projectile release. Marginal performance increases could be obtained by replacing the driver gas with hydrogen.					